WILEY

# Development and validation of tumor-to-blood based nomograms for preoperative prediction of lymph node metastasis in lung cancer

Yili Fu[1] | Xiaoying Xi[2] | Yanhua Tang[3] | Xin Li[1] | Xin Ye[1] | Bin Hu[1] | Yi Liu[1]

[1]Department of Thoracic Surgery, Beijing Chao-Yang Hospital, Beijing, China

[2]Department of Nuclear Medicine, Beijing Chao-Yang Hospital, Beijing, China

[3]Department of Radiology, Beijing Chao-Yang Hospital, Beijing, China

**Correspondence**
Yi Liu, Thoracic Surgery Department, Beijing-Chaoyang Hospital, No 8, Gongti South Road, Chaoyang District, Beijing 100020, China.
Email: drliuyi1987@hotmail.com

## Abstract

**Background:** To develop and validate tumor-to-blood based nomograms for preoperative prediction of lymph node (LN) metastasis in patients with lung cancer (LC).

**Methods:** A prediction model was developed in a primary cohort comprising 330 LN stations from patients with pathologically confirmed LC, these data having been gathered from January 2016 to June 2019. Tumor-to-blood variables of LNs were calculated from positron emission tomography-computed tomography (PET-CT) images of LC and the short axis diameters of LNs were measured on CT images. Tumor-to-blood variables, number of stations suspected of harboring LN metastasis according to PET, and independent clinicopathological risk factors were included in the final nomograms. After being internally validated, the nomograms were used to assess an independent validation cohort containing 101 consecutive LN stations accumulated from July 2019 to March 2020.

**Results:** Four tumor-to-blood variables (left atrium, inferior vena cava, liver, and aortic arch) and the maximum standardized uptake value (SUVmax) for LNs were found to be significantly associated with LN status (p < 0.001 for both primary and validation cohorts). Five predictive nomograms were built. Of these, one with LN SUVmax/left atrium SUVmax was found to be optimal for predicting LN status with AUC 0.830 (95% confidence interval [CI]: 0.774–0.886) in the primary cohort and AUC 0.865 (95% CI: 0.782–0.948) in the validation cohort. All models showed good discrimination, with a modest C-index, and good calibration in both primary and validation cohorts.

**Conclusions:** We have developed tumor-to-blood based nomograms that incorporate identified clinicopathological risk factors and facilitate preoperative prediction of LN metastasis in LC patients.

**KEYWORDS**
blood pool, lung cancer, lymph node metastasis, PET/CT imaging, SUV ratio

## INTRODUCTION

Lung cancer (LC) remains the most common cancer, ranking first as a cause of cancer-related death globally.[1] Accurate identification of lymph node (LN) involvement in lung cancer patients is crucial for successful management.[2,3] Several predictors of LN metastasis have been identified, including LN diameter, tumor differentiation, and tumor size[4,5]; however, they are not very accurate. Differentiating uninvolved LNs from those harboring metastases is critical for pretreatment decision-making regarding the need for adjuvant therapy and the extent of resection.[6]

18F-fluorodeoxyglucose positron emission tomography (18F-FDG PET) plays an important role in identifying LN

status: malignant cells accumulate more FDG than normal tissue because they have a higher metabolic rate.[7,8] Several studies have found that the tumor-to-blood standardized uptake value (SUV) standard uptake ratio (SUR),[9–11] a normalized value of a PET variable relative to blood pool SUV, better predicts LN status than LN maximum standardized uptake value (SUVmax). Although, various PET/CT imaging criteria for malignancy and new variables have been investigated with the aim of improving accuracy, no single predictor for assessing LN status has thus far proved to be reliable.[12,13]

Nomograms have been accepted as preferable and reliable tools for quantitative prediction of risks of malignancy and outcomes.[4,14,15] Combining a number of risk factors, rather than relying on any single one, has been shown to be a viable and dependable approach to making accurate predictions. A few models have been established for predicting LN metastasis in patients with non-small cell lung cancer (NSCLC) on the basis of PET/CT-related variables.[16,17] However, an optimal nomogram that combines multiple clinical factors with SURs has yet to be established. To the best of our knowledge, no published studies have yet determined whether a SUR-based nomogram would more accurately predict LN metastasis in such patients.

Therefore, the aim of this study was to develop and validate a SUR-based nomogram that incorporates clinicopathological risk factors for prediction of LN metastasis in patients with LC.

## METHODS

This retrospective study was approved by the institutional review board of, Beijing, China, and the requirement to obtain informed consent was waived (approval number: 2021-Ke-21).

## Patients

The primary cohort of this study comprised 185 consecutive NSCLC patients with 330 lymph node stations who had undergone PET/CT before resection at the Beijing Chaoyang hospital between January 2016 and June 2019. The model was confirmed using an independent validation cohort comprising 39 patients with 101 resected lymph node stations from July 2019 to March 2020.

The inclusion criteria were as follows: (i) 18F-fluorodeoxyglucose positron emission tomography-computed tomography (PET-CT) performed within the 30 days prior to undergoing resection with curative intent; (ii) no history of other types of cancer; (iii) no neoadjuvant chemotherapy or radiation administered before PET/CT examination; and (iv) systematic lymph node dissection carried out at the second, fourth, seventh, eighth, ninth, 10th and 11th stations for right-sided lung cancers and at the fifth, sixth, seventh, eighth, ninth, 10th and 11th

stations for left-sided lung cancers. The exclusion criteria were as follows: (i) multiple pulmonary nodules, (ii) pure ground-glass opacity (GGO) or part-solid ground-glass opacity (ps-GGO) nodule, (iii) sampling lymph node dissection performed during resection, and (iv) pathological diagnosis of a benign nodule.

Baseline clinicopathological data including age, gender, cell type, data of baseline CT, and smoking status were drawn from the participants' medical records. LN status was defined separately for each LN station. Tumors located centrally were defined as located within the proximal third of the hemithorax; all other tumors were defined as peripheral.

## FDG PET/CT examination

Within 30 days before surgery, all patients underwent PET/CT using an integrated PET/CT scanner (GE Discovery STE) and a standard protocol. Baseline scans of the chest were performed using 5-mm-thick slices. All patients fasted for at least 6 h before the PET/CT examination. The patients' blood glucose concentrations were checked and controlled at <6.8 mmol/L before 18F-fluorodeoxyglucose injection (3.7 to 4.5 MBq/kg bodyweight), which was administered after micturition and resting for 60 min. Images were obtained from the base of the skull to the mid-thigh level.

## Image analysis

Volume viewer software was used to generate volume of interest (VOI) of the tumors and each lymph node station using the threshold SUV. These factors were then used to calculate the SUVmax, average standardized uptake value (SUVave), and tumor volume by drawing a region of interest around it. The SUVmax was defined as the highest voxel within the VOI. SUVave and tumor volume were automatically measured on the workstation, SUV of 40% or greater of the SUVmax being adopted as the threshold.

For the blood pool SUVmax, VOIs were drawn manually on the left atrium, inferior vena cava, liver (1000 mm$^3$) and aortic arch (Figure 1). The blood pool SUVmax and SUVave were automatically measured on the workstation. The SUR was defined as the LN-SUVmax/blood pool. As previously stated, LN status was defined by each LN station, not each patient. The number of suspicious LN stations within each patient was also retrieved. The short axis of each lymph node was measured at the mediastinal window of chest CT images window level 40 HU and window width 350 HU. The equations for each SUR were as follows.

$$SURmax - Lea = \frac{LN\ SUVmax}{Left\ atrium\ SUVmax} \quad (1)$$

$$SURmax - Ivc = \frac{LN\ SUVmax}{Inferior\ vena\ cava\ SUVmax} \quad (2)$$
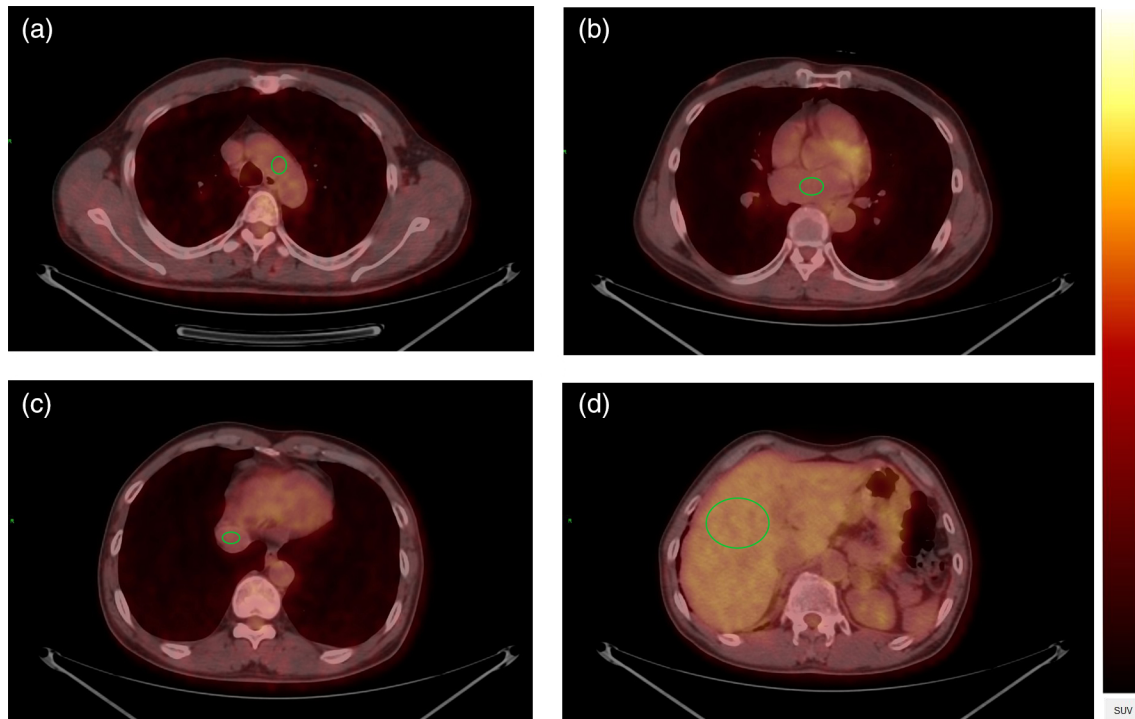
**FIGURE 1** Delineation of arcus aortae, left atrium, inferior vena cava and liver. A roughly circular volume of interest (VOI) was delineated on the positron emission tomography (PET) image (a, arcus aortae, diameter = 1.5 cm; b, left atrium, diameter = 2 cm; c, inferior vena cava, diameter = 1.5 cm; d, liver, area = 1000 mm$^2$) and the margin were excluded

$$SURmax - Liv = \frac{LN\ SUVmax}{Liver\ SUVmax} \quad (3)$$

$$SURmax - Ara = \frac{LN\ SUVmax}{Arcus\ Aortae\ SUVmax} \quad (4)$$

## Comparison of patient characteristics between LN-positive and LN-negative groups and between primary and validation cohorts

Associations between clinicopathological risk factors and LN status and differences in prevalence of affected LNs between the primary and validation cohorts were assessed by univariable analysis.

## Feature selection and prediction model building

We used LN SUVmax and four SURs as the main variables for building five separate models (Models 1–5) for predicting lymph node metastasis. Selected clinical and PET/CT variables were introduced as covariates into each model. Univariate and multivariable logistic regression was performed for all models and an odds ratio (OR) with 95% confidence interval (CI) was used to estimate the strength of correlations. Predictors identified by univariable analysis ($p < 0.05$) were subjected to multivariable regression analysis.

In the primary cohort, multivariable logistic regression analysis began with LN SUVmax, SURmax-Lea, SURmax-Ivc, SURmax-Liv, SURmax-Ara and the remaining selected predictors. Two-way stepwise selection was applied by using the likelihood ratio test with Akaike's information criterion as the stopping rule.[18,19] Numerical and categorical data are presented as mean ± standard deviation and frequency (%), respectively.

## Apparent performance and validation of the nomogram

Calibration curves were plotted to assess calibration of the nomograms by the Hosmer–Lemeshow test.[20] All nomograms were subjected to bootstrapping (1000 bootstrap resamples) to calculate the C-index. The logistic regression formula created in the primary cohort was applied to all patients in the validation cohort; total points for each patient were calculated from factors used in logistic regression in the primary cohort. The C-index and calibration curve were established.

## Decision curve analysis and selection of the optimal nomogram

Decision curves were analyzed to determine the clinical usefulness of all nomograms by quantifying the net benefits at different threshold probabilities in the validation dataset.[21]

Net reclassification improvement (NRI) and integrated discrimination improvement (IDI) were calculated to compare the predictive performance of all models.[22,23] The model with the most modest NRI and IDI was selected as the final model for predicting LN metastasis.

## Statistical analysis

For the clinical and pathological factors, numerical data were analyzed using the Mann–Whitney U test and categorical data by Pearson's $\chi^2$ test. Statistical analysis was conducted with R software (version 4.0.3; http://www.Rproject.org). The reported probabilities are all two-sided with statistical significance set at 0.05.

## RESULTS

On the basis of the selection criteria, a total of 431 LNs in 224 patients were included (Figure 2).

## Patient characteristics

Patient characteristics in the primary and validation cohorts are shown in Table 1. The study cohort comprised 185 patients, of whom 127 were LN-negative and 58 LN-positive. Overall, the 431 LN stations consisted of 69 N1 and 362 N2 stations. There were no significant differences between the two cohorts in LN prevalence (22.7% vs. 30.7%, $p = 0.104$).

## Nomogram model building and selection of the optimal nomogram

Univariate logistic regression identified LN SUVmax, SURmax-Lea, SURmax-Ivc, SURmax-Liv, and SURmax-Ara as independent predictors in the primary cohort. Five models (Models 1–5) were constructed using covariates that were identified as independent predictors by multivariable logistic regression analysis.

Model 2 (SURmax-Lea, LN short axis, tumor volume, suspicious LN stations, tumor location, sex) was found to have a higher C-index in both the primary and validation cohorts than the other models (Table 2). The predictive performance of Model 2 was significantly superior to that of all four other models according to the NRI and IDI (Supplementary Table S1). Therefore Model 2, which incorporates SURmax-Lea, a LN metabolism-related variable, and selected clinical variables, was selected as the optimal model for predicting LN metastases (Figure 3). The results of multivariable logistic regression analysis, C-index and nomograms of Models 1, 3, 4, and 5 are presented as supplementary data (Supplementary Table S1).

## Performance of all nomograms in primary and validation cohorts

The calibration curve in Model 2 for the probability of LN metastasis demonstrated good agreement between prediction and observation in the primary cohort (Figure 4). The Hosmer–Lemeshow test on all nomograms yielded nonsignificant findings, indicating that there was no departure from perfect fit. The calibration curves for Models 1, 3, 4, and 5 are presented as supplementary data (Supplementary Figure S1).

## Clinical use

The decision curve for Model 2 is presented in Figure 5. It shows modest prediction of LN metastasis and that using the nomogram to predict LN metastases is more accurate
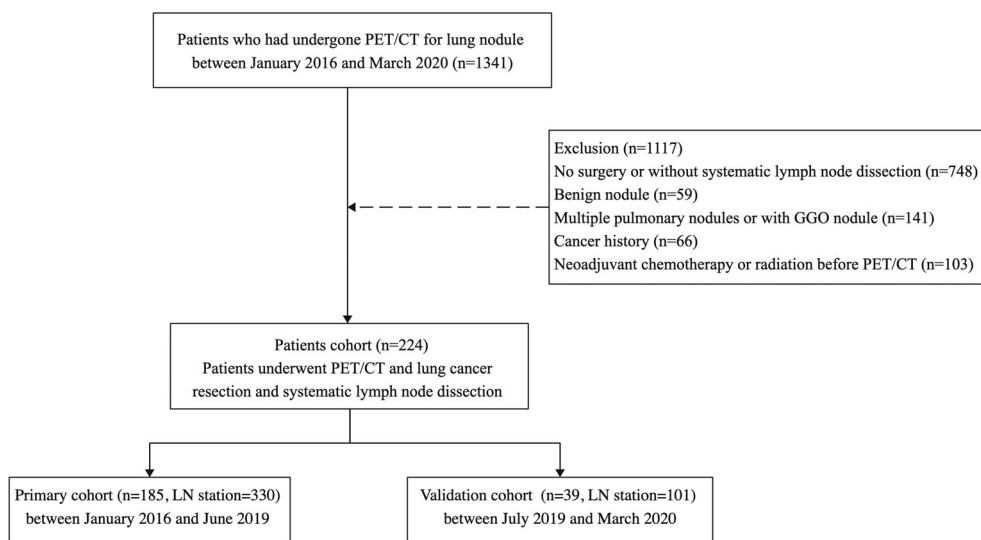


**FIGURE 2** Patient recruitment flowchart

**TABLE 1** Characteristics of patients in the primary and validation cohorts

| Variable | Primary cohort ($n = 330$) | | | Validation cohort ($n = 101$) | | |
|---|---|---|---|---|---|---|
| | LN− ($n = 255$) | LN+ ($n = 75$) | $p$-value | LN− ($n = 70$) | LN+ ($n = 31$) | $p$-value |
| Gender | | | 0.573 | | | 0.668 |
|    Male | 182 (71.4%) | 51 (68.0%) | | 46 (65.7%) | 19 (61.3%) | |
|    Female | 73 (28.6%) | 24 (32.0%) | | 24 (34.3%) | 12 (38.7%) | |
| Age | | | 0.225 | | | 0.013 |
| | 62.5 (10.8) | 61.3 (9.5) | | 62.7 (8.8) | 58.5 (9.0) | |
| Tumor SUVmax | | | <0.001 | | | 0.003 |
| | 7.1 (5.1) | 11.6 (8.1) | | 7.8 (6.2) | 11.0 (4.1) | |
| Tumor volume | | | 0.004 | | | 0.001 |
| | 11.2 (11.4) | 18.2 (19.4) | | 16.2 (19.8) | 37.6 (33.4) | |
| Tumor location | | | <0.001 | | | 0.006 |
|    Peripheral | 153 (60.0%) | 25 (33.3%) | | 41 (58.6%) | 9 (29.0%) | |
|    Central | 102 (40.0%) | 50 (66.7%) | | 29 (41.4%) | 22 (71.0%) | |
| LN SUVmax | | | <0.001 | | | <0.001 |
| | 2.2 (1.5) | 4.8 (3.7) | | 2.1 (1.7) | 4.9 (4.4) | |
| LN SUVave | | | <0.001 | | | <0.001 |
| | 1.7 (0.8) | 3.2 (2.2) | | 1.8 (1.1) | 3.2 (2.7) | |
| LN short axis (mm) | | | <0.001 | | | 0.004 |
| | 5.8 (1.8) | 7.7 (2.9) | | 5.1 (1.6) | 7.1 (3.4) | |
| SURmax-Lea | | | <0.001 | | | <0.001 |
| | 1.3 (1.0) | 3.3 (2.7) | | 1.2 (1.1) | 3.2 (2.9) | |
| SURmax-Ivc | | | <0.001 | | | <0.001 |
| | 1.4 (1.2) | 3.3 (2.7) | | 1.5 (1.6) | 3.8 (3.7) | |
| SURmax-Liv | | | <0.001 | | | <0.001 |
| | 0.8 (0.6) | 1.8 (1.4) | | 0.7 (0.6) | 1.8 (1.8) | |
| SURmax-Ara | | | <0.001 | | | <0.001 |
| | 1.4 (1.1) | 3.2 (2.6) | | 1.4 (1.4) | 3.3 (2.9) | |
| Cell type | | | 0.230 | | | 0.297 |
|    Adenocarcinoma | 153 (60.0%) | 47 (62.7%) | | 35 (50.0%) | 13 (41.9%) | |
|    Squamous cell carcinoma | 72 (28.2%) | 15 (20.0%) | | 29 (41.4%) | 12 (38.7%) | |
|    Other | 30 (11.8%) | 13 (17.3%) | | 6 (8.6%) | 6 (19.4%) | |
| Smoking status | | | 0.686 | | | 0.489 |
|    Current | 83 (32.5%) | 27 (36.0%) | | 17 (24.3%) | 5 (16.1%) | |
|    Former | 59 (23.1%) | 19 (25.3%) | | 12 (17.1%) | 4 (12.9%) | |
|    Never | 113 (44.3%) | 29 (38.7%) | | 41 (58.6%) | 22 (71.0%) | |
| Suspicious LN metastasis | | | 0.013 | | | 0.017 |
|    <2 stations | 92 (36.1%) | 39 (52.0%) | | 23 (32.9%) | 18 (58.1%) | |
|    >=2 stations | 163 (63.9%) | 36 (48.0%) | | 47 (67.1%) | 13 (41.9%) | |

*Note*: The $p$-value is derived from the univariable association analyses between each of the clinicopathological variables and LN status.

Abbreviations: LN, lymph node; LN−, lymph node negative; LN+, lymph node metastasis; mm, millimeter; SUVave, average standardized uptake value; SUVmax, maximum standardized uptake value.

than either the treat-all-patients or the treat-none scheme; however, there were several overlaps between the models. The decision curves for the other four models are presented as supplementary data (Figure S2).

## DISCUSSION

We developed and validated five different LN SUVmax-based nomograms for preoperative prediction of LN

metastasis in patients with lung cancer. All nomograms successfully stratified patients according to their risk of LN metastases, SURmax-Lea being the most accurate of the models. Incorporating variables related to LN metabolism and clinical risk factors into a usable nomogram facilitated preoperative prediction of LN metastasis.

Unlike previous studies[4,5,10,24] that reported means of predicting LN metastases in a given individual, we used LN SUVmax of each station to predict metastases in the corresponding LN station when constructing all of our models. Using only the LN station with the highest SUVmax is arbitrary and potentially inaccurate because a single individual may have multiple LNs with abnormal SUVmax. Furthermore, a high LN SUVmax is not diagnostic of the presence of metastasis and vice versa. In the present study, 11 patients (18.9%) with low LN SUVmax had LN metastases, whereas some cases with higher SUVmax did not. Use of only the highest LN SUVmax for prediction would have yielded a greater proportion of false negatives, blunting the accuracy of prediction.

The tumor-to-background ratio has been widely used to differentiate between benign and malignant status, especially regarding tumors with low metabolic rates, because it balances each individual's background by incorporating a blood pool value.[5,12,25] Most tumor-to-background ratio studies, including those on colorectal, rectal, and esophageal cancer, have demonstrated a modest ability to differentiate cancer.[4,13,26] However, no previous studies have compared different blood pools and identified which is optimal for prediction.

We used the left atrium, inferior vena cava, liver, and aortic arch as blood pools when constructing our models for determining LN metastatic status. The aortic arch and liver have been selected as background blood pools in many previous studies on prediction of LN status,[12,13,26,27] whereas, to the best of our knowledge, no previous studies have used the left atrium or inferior vena cava for this purpose. According to univariable analysis, predictions by LN SUVmax and four SURs were of comparable accuracy; however, the differences between them widened when we integrated all clinical factors into the models. Although there were no differences between the four blood pool baselines, SUR-Lea combined with multiple clinical factors was superior to all of the other models in classifying LN metastasis status. The reclassification performance was better than that of the other prediction models, with significant NRI and IDI. This superior accuracy may be attributable to the addition of one more predictor, sex, to the SUR-Lea based model. Among all five models, the ROC showed significant superiority over LN SUVmax for prediction only (NRI, 0.236, 0.256, 0.048, 0.089 and 0.132, $p < 0.01$).

Some published studies have shown that carcinoembryonic antigen (CEA) can serve as an important predictor of LN metastases.[17] However, we did not include

**TABLE 2** Risk factors of all models for lymph node metastasis in lung cancer

| Variable | Model 2 | | |
| --- | --- | --- | --- |
| | ß | Odds ratio (95% CI) | p-value |
| SURmax-Lea | 1.875 | 1.438–2.445 | <0.0001 |
| LN short axis | 1.214 | 1.042–1.415 | 0.013 |
| Tumor volume | 1.023 | 1.001–1.045 | 0.042 |
| Tumor location | 2.130 | 1.127–4.023 | 0.011 |
| Suspicious LN metastasis | 2.265 | 1.204–4.259 | 0.015 |
| Gender | 1.955 | 1.00–3.822 | 0.048 |
| C-index | | | |
| Primary cohort | 0.830 | 0.774–0.886 | 0.001 |
| Validation cohort | 0.875 | 0.782–0.948 | 0.001 |

*Note:* ß is the regression coefficient. *p*-value, odds ratio and confidence interval were derived from the multivariable regression. In net reclassification index and integrated discrimination improvement analysis, model 1 was regard as reference and compared to other four models.

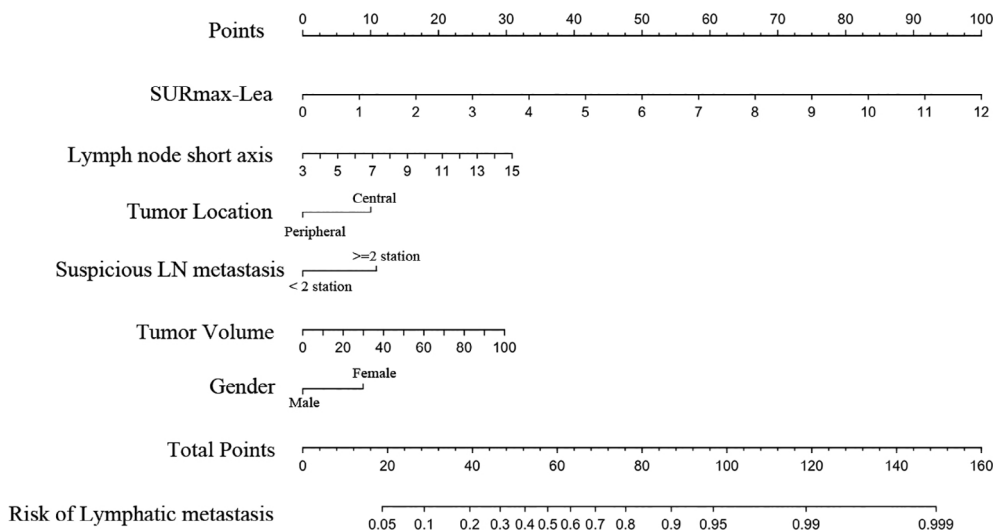Abbreviations: CI, confidence interval; LN, lymph node; SUVmax, maximum standardized uptake value.



**FIGURE 3** Developed nomogram of SURmax-Lea and clinic predictors. The SURmax-Lea, LN short axis, tumor volume, tumor location, suspicious LN metastasis and gender were incorporated in this nomogram

**FIGURE 4** Calibration curves of the SURmax-Lea nomograms in the primary cohort. The predictors include SURmax-lea, LN short axis, tumor volume, tumor location, suspicious LN metastasis and gender. The x-axis represents the predicted LN metastasis risk. The diagonal dotted line represents a perfect prediction by an ideal model. The solid line represents the performance of the nomogram, of which a closer fit to the diagonal dotted line represents a better prediction
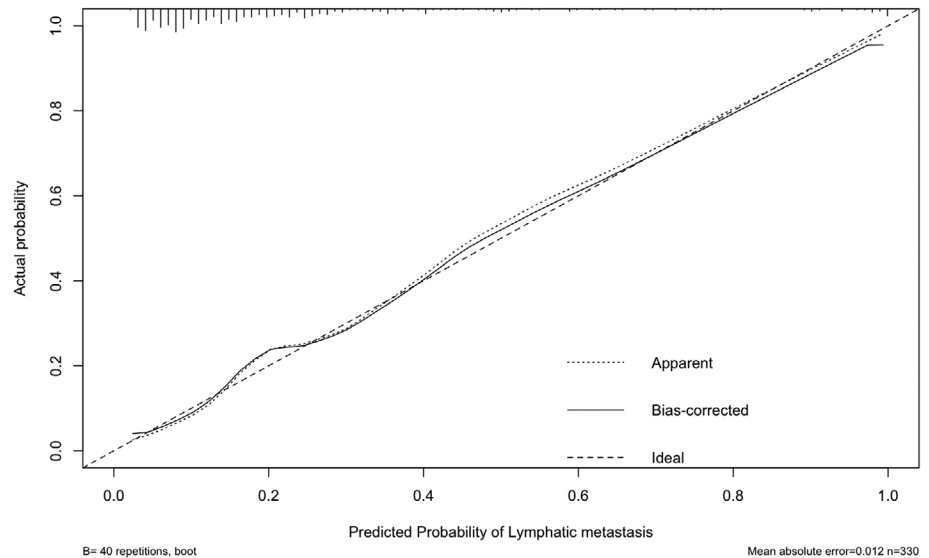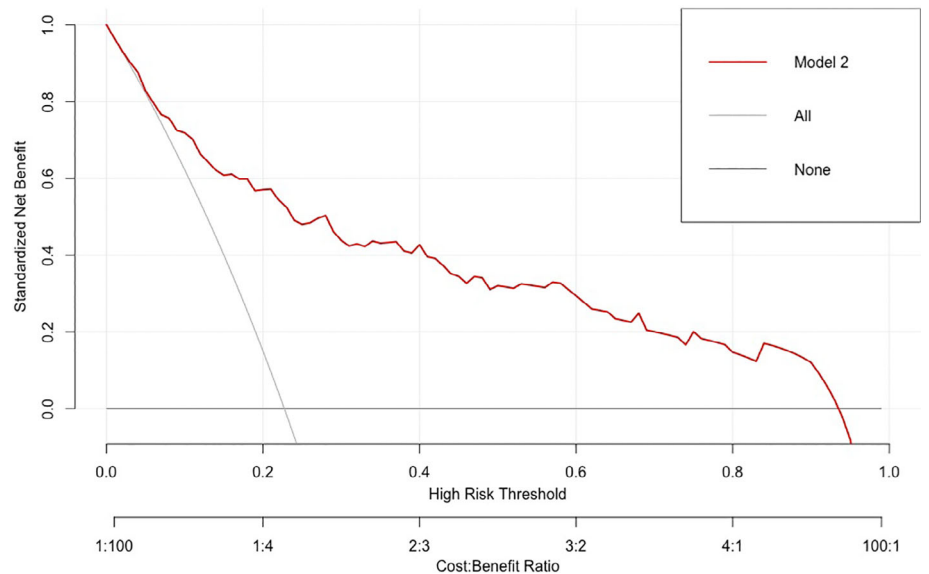
**FIGURE 5** Decision curve analysis for SURmax-Lea nomograms. The y-axis measures the net benefit. The red line represents the nomogram. The gray line represents the assumption that all patients have LN metastases. Thin black solid line represents the assumption that no patients have LN metastases

CEA concentration in our models because we were determining LN status by station, not individually. If we had incorporated it, the false positive rate would have increased for LN stations without metastases and with low SUVmax in patients with high CEA concentrations that were attributable to LN metastases elsewhere. Therefore, adding CEA concentrations to our models would inevitably have augmented bias and reduced the diagnostic accuracy.

Whether the number of LN stations suspected on the basis of radiological findings of harboring metastases is an independent risk factor for LN metastasis is of interest. No previous studies have used this as a predictor. Unsurprisingly, on the one hand, in our study, univariable analysis identified such suspected metastases as a significant predictor ($p < 0.001$). On the other hand, incorporation of radiologically-suspected LN metastasis did not improve the reclassification performance in Models 3 and 5. Its inclusion may have introduced

multicollinearity between LN SUVmax-related variables and LN stations suspected of harboring metastases.

In this study, the N1 station was not separated from the N2 station in primary and the validation cohort because of the limited numbers (69 N1 LN stations). It was difficult to distinguish metastatic hilar and interlobar lymph nodes from those which were negative because of the soft-tissue character and proximity to the bronchus.[28,29] The diagnostic accuracy of PET/CT for detecting N1 LN metastasis is fair but has a high false negative rate.[30] In order to increase the diagnostic accuracy of metastatic N1 LNs, endobronchial ultrasound (EBUS) or endoscopic ultrasound fine needle aspiration (EUS-FNS) combined PET/CT are recommended for the detection of metastatic N1 LNs in CT or PET-CT negative LNs.[31]

Limitations of our study include its small size. Only 185 patients with 431 LN stations were included; this may

have introduced bias. Furthermore, the SUVmax of N1 station was not routinely measured, being determined only when there was evidence of hypermetabolism, resulting in an imbalance between the number of N1 and N2 stations. In addition, we were unable to include genomic characteristics because this was a retrospective study. In future, identification of reliable gene markers may contribute to building a more accurate prediction model.

In conclusion, this study presents five models that incorporate both metabolism signatures and clinical risk factors. These may facilitate the individualized prediction of LN metastasis in patients with lung cancer.

## ORCID
*Yili Fu* 🔟 https://orcid.org/0000-0002-9806-615X
*Xin Li* 🔟 https://orcid.org/0000-0002-9064-5114
*Yi Liu* 🔟 https://orcid.org/0000-0003-3237-2362

## REFERENCES

1. Sung H, Ferlay J, Siegel RL, Laversanne M, Soerjomataram I, Jemal A, et al. Global cancer statistics 2020: GLOBOCAN estimates of incidence and mortality worldwide for 36 cancers in 185 countries. CA Cancer J Clin. 2021;71:209–249.
2. Smeltzer MP, Faris NR, Ray MA, Osarogiagbon RU. Association of pathologic nodal staging quality with survival among patients with non-small cell lung cancer after resection with curative intent. JAMA Oncol. 2018;4:80–7.
3. Asamura H, Chansky K, Crowley J, Goldstraw P, Rusch VW, Vansteenkiste JF, et al. The International Association for the Study of Lung Cancer lung cancer staging project: proposals for the revision of the N descriptors in the forthcoming 8th edition of the TNM classification for lung cancer. J Thorac Oncol. 2015;10:1675–84.
4. Huang YQ, Liang CH, He L, Tian J, Liang CS, Chen X, et al. Development and validation of a radiomics nomogram for preoperative prediction of lymph node metastasis in colorectal cancer. J Clin Oncol. 2016;34:2157–64.
5. Ouyang ML, Tang K, Xu MM, Lin J, Li TC, Zheng XW. Prediction of occult lymph node metastasis using tumor-to-blood standardized uptake ratio and metabolic parameters in clinical N0 lung adenocarcinoma. Clin Nucl Med. 2018;43:715–20.
6. Ettinger DS, Wood DE, Aisner DL, Akerley W, Bauman JR, Bharat A, et al. NCCN guidelines insights: non-small cell lung cancer, version 2.2021. J Natl Compr Canc Netw. 2021;19:254–66.
7. Guo HY, Lin JT, Huang HH, Gao Y, Yan MR, Sun M, et al. Development and validation of a (18)F-FDG PET/CT-based clinical prediction model for estimating malignancy in solid pulmonary nodules based on a population with high prevalence of malignancy. Clin Lung Cancer. 2020;21:47–55.
8. Ouyang ML, Xia HW, Xu MM, Lin J, Wang LL, Zheng XW, et al. Prediction of occult lymph node metastasis using SUV, volumetric parameters and intratumoral heterogeneity of the primary tumor in T1-2N0M0 lung cancer patients staged by PET/CT. Ann Nucl Med. 2019;33:671–80.
9. Chong GO, Jeong SY, Lee YH, Park SH, Lee HJ, Hong DG, et al. Improving the prognostic performance of SUVmax in 18F-fluorodeoxyglucose positron-emission tomography/computed tomography using tumor-to-liver and tumor-to-blood standard uptake ratio for locally advanced cervical cancer treated with concurrent chemoradiotherapy. J Clin Med. 2020;9:1878.
10. Cho J, Choe JG, Pahk K, Choi S, Kwon HR, Eo JS, et al. Ratio of mediastinal lymph node SUV to primary tumor SUV in (18)F-FDG PET/CT for nodal staging in non-small-cell lung cancer. Nucl Med Mol Imaging. 2017;51:140–6.
11. Mattes MD, Moshchinsky AB, Ahsanuddin S, Rizk NP, Foster A, Wu AJ, et al. Ratio of lymph node to primary tumor SUV on PET/CT accurately predicts nodal malignancy in non-small-cell lung cancer. Clin Lung Cancer. 2015;16:e253–8.
12. Hofheinz F, Hoff J, Steffen IG, Lougovski A, Ego K, Amthauer H, et al. Comparative evaluation of SUV, tumor-to-blood standard uptake ratio (SUR), and dual time point measurements for assessment of the metabolic uptake rate in FDG PET. EJNMMI Res. 2016;6:53.
13. Belge G, Bilgin C, Ozkaya G, Kandemirli SG, Alper E. Prognostic value of pretreatment tumor-to-blood standardized uptake ratio (SUR) in rectal cancer. Ann Nucl Med. 2020;34:432–40.
14. Rose PG, Java J, Whitney CW, Stehman FB, Lanciano R, Thomas GM, et al. Nomograms predicting progression-free survival, overall survival, and pelvic recurrence in locally advanced cervical cancer developed from an analysis of identifiable prognostic factors in patients from NRG oncology/gynecologic oncology group randomized trials of chemoradiotherapy. J Clin Oncol. 2015;33:2136–42.
15. Balachandran VP, Gonen M, Smith JJ, DeMatteo RP. Nomograms in oncology: more than meets the eye. Lancet Oncol. 2015;16:e173–80.
16. Xie Y, Zhao H, Guo Y, Meng F, Liu X, Zhang Y, et al. A PET/CT nomogram incorporating SUVmax and CT radiomics for preoperative nodal staging in non-small cell lung cancer. Eur Radiol. 2021.
17. Nie P, Yang G, Wang N, Yan L, Miao W, Duan Y, et al. Additional value of metabolic parameters to PET/CT-based radiomics nomogram in predicting lymphovascular invasion and outcome in lung adenocarcinoma. Eur J Nucl Med Mol Imaging. 2021;48:217–30.
18. Collins GS, Reitsma JB, Altman DG, Moons KGM. Transparent reporting of a multivariable prediction model for individual prognosis or diagnosis (TRIPOD): the TRIPOD statement. BMJ. 2015;350: g7594.
19. Sauerbrei W, Boulesteix AL, Binder H. Stability investigations of multivariable regression models derived from low- and high-dimensional data. Journal of Biopharmaceutical Statistics. 2011;21:1206–1231.
20. Kramer AA, Zimmerman JE. Assessing the calibration of mortality benchmarks in critical care: the Hosmer-Lemeshow test revisited. Crit Care Med. 2007;35:2052–6.
21. Vickers AJ, Cronin AM, Elkin EB, Gonen M. Extensions to decision curve analysis, a novel method for evaluating diagnostic tests, prediction models and molecular markers. BMC Med Inform Decis Mak. 2008;8:53.
22. Tangri N, Stevens LA, Griffith J, Tighiouart H, Djurdjev O, Naimark D, et al. A predictive model for progression of chronic kidney disease to kidney failure. JAMA. 2011;305:1553–9.
23. Pencina MJ, D'Agostino RB Sr, Steyerberg EW. Extensions of net reclassification improvement calculations to measure usefulness of new biomarkers. Stat Med. 2011;30:11–21.
24. Farjah F, Lou F, Sima C, Rusch VW, Rizk NP. A prediction model for pathologic N2 disease in lung cancer patients with a negative mediastinum by positron emission tomography. J Thorac Oncol. 2013;8: 1170–80.
25. Hofheinz F, Butof R, Apostolova I, Zophel K, Steffen IG, Amthauer H, et al. An investigation of the relation between tumor-to-liver ratio (TLR) and tumor-to-blood standard uptake ratio (SUR) in oncological FDG PET. EJNMMI Res. 2016;6:19.
26. Butof R, Hofheinz F, Zophel K, Stadelmann T, Schmollack J, Jentsch C, et al. Prognostic value of Pretherapeutic tumor-to-blood

standardized uptake ratio in patients with esophageal carcinoma. J Nucl Med. 2015;56:1150–6.

27. Boktor RR, Walker G, Stacey R, Gledhill S, Pitman AG. Reference range for intrapatient variability in blood-pool and liver SUV for 18F-FDG PET. J Nucl Med. 2013;54:677–82.

28. Dyas AR, King RW, Ghanim AF, Cerfolio RJ. Clinical Misstagings and risk factors of occult nodal disease in non-small cell lung cancer. Ann Thorac Surg. 2018;106:1492–8.

29. Lim CH, Ahn TR, Moon SH, Cho YS, Choi JY, Kim BT, et al. PET/CT features discriminate risk of metastasis among single-bone FDG lesions detected in newly diagnosed non-small-cell lung cancer patients. Eur Radiol. 2019;29:1903–11.

30. Serra P, Centeno C, Sanz-Santos J, Torky M, Baeza S, Mendiluce L, et al. Is it necessary to sample the contralateral nodal stations by EBUS-TBNA in patients with lung cancer and clinical N0/N1 on PET-CT? Lung Cancer J Iaslc. 2020;142:9–12.

31. Hegde P, Molina JC, Thivierge-Southidara M, Jain RV, Gowda A, Ferraro P, et al. Combined endosonographic mediastinal lymph node staging in positron emission tomography and computed tomography node-negative non-small-cell lung cancer in high-risk patients. Semin Thorac Cardiovasc. 2020;32:162–8.

## SUPPORTING INFORMATION

Additional supporting information may be found online in the Supporting Information section at the end of this article.

---

**How to cite this article:** Fu Y, Xi X, Tang Y, et al. Development and validation of tumor-to-blood based nomograms for preoperative prediction of lymph node metastasis in lung cancer. Thorac Cancer. 2021; 12:2189–2197. https://doi.org/10.1111/1759-7714. 14066